doi: 10.32023/0001-5237/72.3.5

ACTA ASTRONOMICA
Vol. **72** (2022) pp. 233–243

On the Relation between OH and CH Radicals, Molecular/Neutral Hydrogen and Major 5780/5797 Diffuse Interstellar Bands

T. W e s e l a k

Institute of Physics, Kazimierz Wielki University, Powst. Wielkopolskich 2,
85-072 Bydgoszcz, Poland

Received July 7, 2022

ABSTRACT

A precise relation between column densities of OH and CH molecule in the ISM has been found based on spectra of 24 stars (four of them new) and new published oscillator strengths of lines near 3078 Å and 3082 Å of OH molecule (0.001007 and 0.0006226, respectively). Observed column density ratio of OH and CH molecules in the ISM is equal to 3.20 ± 0.17. A very good relation (with correlation coefficient equal to 0.85) between abundances of OH molecule and molecular hydrogen is also presented.

Key words: *ISM: clouds – ISM: molecules*

1. Introduction

Interstellar hydrides, *i.e.*, molecules or molecular ions containing a single heavy element with one or more hydrogen atom, are valuable probes of interstellar medium. Seven neutral diatomic hydrides have previously been detected in the interstellar clouds – CH (Swings and Rosenfeld 1937), OH (Weinreb *et al.* 1963), HCl (Blake *et al.* 1985), NH (Meyer and Roth 1991), HF (Neufeld *et al.* 1997), SiH (Schilke *et al.* 2001) and SH (Neufeld *et al.* 2012) – also with five diatomic hydrine cations – CH^+ (Douglas and Herzberg 1941), OH^+ (Wyrowski *et al.* 2010), SH^+ (Benz *et al.* 2010), HCl^+ (De Luca *et al.* 2012) and ArH^+ (Schilke *et al.* 2014). Four discoveries of interstellar hydrides were made with Herschel (SH^+, HCl^+, ArH^+, OH^+) and one (SH) with SOFIA instruments (see Gerin *et al.* 2016 as a review).

The hydroxyl radical (OH) transition was detected at 18 cm band in the interstellar medium (ISM) by Weinreb *et al.* (1963). Later, its electronic tranitions were identified in ultraviolet spectra of bright OB-stars (Crutcher and Watson 1976, Chaffee and Lutz 1977, Felenbok and Roueff 1996). Recently, two lines resulting from electronic transitions of the $A^2\Sigma^+ - X^2\Pi_i$ band (near 3078 Å and 3082 Å), were used to obtain column densities toward 16 translucent sightlines (Weselak *et al.* 2010b). Determinations of OH column densities are based on oscillator

strengths which were reanalyzed by Roueff (1996). However, new precise values of oscillator strengths of OH electronic transitions of the $A^2\Sigma^+ - X^2\Pi_i$ band have recently been published by Yousefi *et al.* (2018).

Interstellar lines of CH molecule were identified by McKellar (1940ab) in spectra of OB stars due to its A–X feature centered near 4300 Å as the strongest observed interstellar line in the violet region. However, this line is frequently saturated. Since the B–X system near 3886 Å is also quite frequently observed and being much weaker than the A–X one it is almost always unsaturated. Also unsaturated is the B–X system near 3633 Å which is less frequently observed. Abundances of the CH molecule were proved to be very tightly correlated with those of H_2 molecule (*e.g.*, Federman 1982, Mattila 1986, Sheffer *et al.* 2008). The oscillator strengths of CH transitions were extensively analyzed by Lien (1984) and Weselak *et al.* (2011, 2014).

Here we extend the above mentioned sample (Weselak *et al.* 2010b) of the UV OH absorption bands adding ground-based observations, done using the high-resolution UVES spectrograph toward three new targets (HD 147933, HD 172028, HD 210121) from the work of Bhatt and Cami (2015). Data on HD 62542 are from the work of Welty *et al.* (2020). The aim of this work is to investigate relations between column densities of the OH (based on new values of oscillator strengths) and CH molecules and test oscillator strengths of OH A–X and CH B–X (0,0) and (1,0) transitions based on unsaturated lines at 3078 Å, 3082 Å and 3886 Å, 3890 Å and 3633 Å, 3636 Å, respectively. All the observed features of diatomic molecules are presented in Table 1 with position and oscillator strength taken from the literature.

T a b l e 1

Adopted molecular parameters

Species	Vibronic band	Rotational lines	Position [Å]	Ref.	f-value	Ref.
OH	$A^2\Sigma^+$–$X^2\Pi_i$ (0,0)	$Q_1(3/2)+{}^QP_{21}(3/2)$	3078.443	1	0.0010070	2
	(0,0)	$P_1(3/2)$	3081.6645	1	0.0006226	2
CH	$B^2\Sigma^-$–$X^2\Pi$ (0,0)	$Q_2(1)+{}^QR_{12}(1)$	3886.409	3	0.00320	4
	(0,0)	${}^PQ_{12}(1)$	3890.217	3	0.00213	4
	$B^2\Sigma^-$–$X^2\Pi$ (1,0)	$Q_2(1)+{}^QR_{12}(1)$	3633.289	5	0.00104	5
	(1,0)	${}^PQ_{12}(1)$	3636.222	5	0.00069	5

References: 1 – Weselak *et al.* (2009), 2 – Yousefi *et al.* (2018), 3 – Gredel *et al.* (1993), 4 – Lien (1984), 5 – Weselak *et al.* (2011)

The results from the Copernicus satellite showed that the H_2 molecule is relatively rich in diffuse and translucent clouds (Savage *et al.* 1977) with abundances exceeding 10^{19} cm^{-2} toward OB stars. This result was also proven by another set of column densities, based on the data acquired with the FUSE satellite (Rachford *et al.* 2002, 2009, Pan *et al.* 2004, Snow *et al.* 2008).

Since the discovery of two major diffuse interstellar bands (DIBs) at 5780 Å and 5797 Å (Heger 1922) the number of known DIBs has grown up to the current number of more than 400 entries (Hobbs *et al.* 2009). However, the problem of their origin remains unsolved. Close connections of simple molecular species to strong 5780 and 5797 DIBs suggest their molecular origin (Sheffer *et al.* 2008, Weselak *et al.* 2008, 2010a, Weselak 2019, 2020). In this paper we also present relations between column densities of OH and intensities of major 5780 and 5797 diffuse bands (not presented previously).

2. Observational Data

For this project we used the sample of 24 early type stars in spectra of which features of OH (near 3078 Å and 3082 Å) and CH (near 3886 Å and 3890 Å and near 3633 Å and 3636Å) were accessible.

T a b l e 2

Column densities of interstellar features [10^{12} cm^{-2}]

HD	Spec.	$E(B-V)$	N(OH)	N(CH)	N(H_2)	N(HI)	$r_{H2/HI}$	W(5780)	W(5797)	ref
23180	B1III	0.27	82.89 ± 18.4^{p}	22.24 ± 2.91	4	7.94	a/a	90.6 ± 1.5	66.2 ± 1.9	b
24398	B1Iab	0.29	40.99 ± 1.32^{q}	22.3 ± 2.61	4.7	6.45	a/a	99 ± 1.9	58.4 ± 1.7	b
27778	B3V	0.37	104.8 ± 2.55^{q}	39.93 ± 4.1	6.17	9.54	c/c	91.8 ± 1.6	42.2 ± 1.1	b
34078	O9.5Ve	0.49	36.8 ± 5.01^{r}	79.27 ± 4.82	6.4	15.85	d/e	178 ± 3.6	63 ± 5	b
62542	B3V	0.35	111.8 ± 8.74^{f}	26.58 ± 4.62	6.46		f	35.4	14.5	g
110432^{v}	B2pe	0.48	45.9 ± 7.91	18.12 ± 0.28	4.37	7.08	c/h	140.8 ± 3.7	39.8 ± 3.1	b
147889^{v}	B2III/IV	1.02	314.2 ± 30.8	100.51 ± 14.25		63.1	g	370 ± 4.7	152 ± 4.3	k
147933	B2IV	0.48	81.59 ± 6.53^{s}	18.73 ± 1.18	3.71	42.65	a/a	206.8	57.8	g
148688^{v}	B1Ia	0.55	28.51 ± 11.26	9.29 ± 1.68				343 ± 9	85.2 ± 2.5	k
149757^{v}	O9.5V	0.28	50.67 ± 9.87	24.89 ± 2.92	4.4	5.26	a/a	72.7 ± 1.1	35.5 ± 0.9	b
151932^{v}	WN7	0.50	83.45 ± 6.89	30.35 ± 5.8						
152236^{v}	B1 Iape	0.66	87.5 ± 8.13	27.24 ± 0.72	5.37	58.88	c/d	340.5 ± 4.8	101.8 ± 3.2	b
152249^{v}	O9Ib	0.48	68.06 ± 18.87	17.23 ± 1.39				242 ± 3.8		k
152270^{v}	WC7	0.50	51.76 ± 14.92	17.79 ± 2.61						
154368^{v}	O9Ia	0.80	197.36 ± 21.24	62.25 ± 5.44	14.45	10	m/m	206.1 ± 4.2	104.2 ± 3.1	b
154445^{v}	B1V	0.35	52.85 ± 7.08	21.72 ± 2.7				192 ± 3.9	62.1 ± 1.9	k
154811^{v}	O9.5Ib	0.66	60.12 ± 12.37	22.85 ± 2.79						
161056^{v}	B1V	0.60	200.52 ± 15.31	58.3 ± 7.44		16.98	n			
163800^{v}	O7	0.57	87.84 ± 17.3	36.43 ± 5.52				256 ± 2	107 ± 1.5	k
164794^{v}	O4V	0.36	37.47 ± 12.84	11.86 ± 2.47	1.26	19.49	g/g	154 ± 2.3	40.3 ± 1.4	k
169454^{v}	B1Ia	1.1	118.01 ± 16.62	45.82 ± 6.53	9.55	32.36	g/g	497.7 ± 2	196.7 ± 1.6	g
170740^{v}	B2V	0.45	56.39 ± 7.64	19.91 ± 6.78	7.24	10.71	g/g	$247.8 \pm 1.$	75 ± 0.2	g
172028	B3II/III	0.79	137.96 ± 8.73^{s}	47.83 ± 3.4				256 ± 8	217 ± 5	o
210121	B7II	0.32	110.6 ± 6.17^{s}	26.65 ± 2.25	5.62	4.26	g/g	70 ± 7	46 ± 9	o

References: a – Savage *et al.* (1977), b – Weselak (2019), c – Rachford *et al.* (2002), d – Sheffer *et al.* (2007), e – Fitzpatrick and Massa (1990), f – Welty *et al.* (2020), g – Fan *et al.* (2017), h – Rachford *et al.* (2001), k – Weselak *et al.* (2008), l – Diplas and Savage (1994), m – Snow (1996) n – Cox *et al.* (2017), o – Friedman *et al.* (2011), p – Roueff (1996), q – Felenbok and Roueff (1996), r – Boissé *et al.* (2005), s – Bhatt and Cami (2015). Equivalent widths of 5780 and 5797 DIBs are in mÅ. Observational data from UVES are designed with *v*

Most of our observational material, presented in Table 2, was obtained using the UVES spectrograph at the ESO Paranal Observatory in Chile with the resolution $R = 80\,000$. These spectra cover the range from 3040 Å to 10 400 Å. They were acquired as a part of the "Library of High-Resolution Spectra of Stars across the Hertzsbrung-Russell Diagram" and are available at the website:
http://www.sc.eso.org/santiago/uvespop.
For more information see Bagnulo *et al.* (2003). These are the spectra in which direct measurements of all molecular species of interest are available. All the spectra were reduced using the standard packages MIDAS and IRAF, as well as DECH code (Galazutdinov 1992), which provides all the standard procedures of image and spectra processing.

In the cases of objects where we found no UVES spectra we took the OH band intensities from the literature and the intensities of other molecular features from our own observations. This was in case of eight objects (OH A–X (0,0) band) and three objects (CH B–X (1,0) band) presented in Table 2.

Table 2 presents column density of each molecule, *i.e.*, OH (based on A–X band), CH (based on B–X (0,0) and B–X (1,0) bands), column density of molecular (H_2) and atomic hydrogen (HI) and equivalent widths of 5780 and 5797 DIB taken from the literature.

T a b l e 3

Measured equivalent widths of interstellar features of OH and CH molecules [mÅ]

HD	W(OH_{3078})	W(OH_{3082})	W(CH_{3886})	W(CH_{3889})	N(CH BX(0,0))	W(CH_{3633})	W(CH_{3636})	N(CH BX(1,0))
23180	3.5 ± 1.1		4.51 ± 0.56	3.29 ± 0.45	22.24 ± 2.91			
24398	1.67 ± 0.08	1.11 ± 0.05	4.96 ± 0.5	3.01 ± 0.38	22.3 ± 2.61			
27778	5.3 ± 0.15	2.2 ± 0.1	9.75 ± 0.78	4.82 ± 0.64	39.93 ± 4.1			
34078	1.72 ± 0.27	0.86 ± 0.21	16.75 ± 1.3	11.28 ± 0.5	79.27 ± 4.82			
62542[a]	4.6 ± 0.4	3 ± 0.4	7.2 ± 0.4	4.9 ± 0.6	34.26 ± 3.77			
110432[v]	1.81 ± 0.41	1.28 ± 0.34	4.1 ± 0.2	2.4 ± 0.2	18.12 ± 0.28	1.21 ± 0.13	0.71 ± 0.12	17.91 ± 0.61
147889[v]	13.8 ± 1.74	7.89 ± 1.68	20.07 ± 1.2	15.02 ± 0.98	100.13 ± 5.87	6.07 ± 0.64	4.05 ± 0.58	100.88 ± 12.99
147933[b]	3.63 ± 0.27	2.02 ± 0.31				1.23 ± 0.09	0.63 ± 0.07	18.57 ± 1.68
148688	1.1 ± 0.45	0.81 ± 0.54	3.83 ± 0.2	2.75 ± 0.2	18.73 ± 1.18			
149757[v]	2.06 ± 0.67	1.30 ± 0.32	5.45 ± 0.2	3.57 ± 0.1	25.44 ± 0.82	1.49 ± 0.13	0.96 ± 0.13	24.33 ± 2.8
151932[v]	3.88 ± 0.71	2.13 ± 0.54	5.97 ± 0.78	3.6 ± 0.45	26.76 ± 3.42	2.23 ± 0.23	1.24 ± 0.21	33.94 ± 4.69
152236[v]	3.5 ± 0.44	2.41 ± 0.34	5.34 ± 0.45	4.15 ± 0.56	27.05 ± 3.1			
152249[v]	2.81 ± 1	1.82 ± 0.8	3.4 ± 0.5	2.61 ± 0.4	17.23 ± 1.39			
152270[v]	1.95 ± 0.64	1.5 ± 0.7	3.52 ± 0.43	2.69 ± 0.45	17.79 ± 2.61			
154368[v]	8.21 ± 1.2	5.24 ± 0.86	12.24 ± 1.1	9.32 ± 0.4	61.75 ± 4.1	3.76 ± 0.16	2.53 ± 0.17	62.75 ± 3.57
154445[v]	2.01 ± 0.31	1.52 ± 0.33	4.06 ± 0.2	2.84 ± 0.2	19.59 ± 0.39	1.34 ± 0.13	1.02 ± 0.12	23.85 ± 2.67
154811[v]	2.43 ± 0.70	1.64 ± 0.5	5.03 ± 0.34	3.12 ± 0.56	22.85 ± 2.79			
161056[v]	8.38 ± 0.77	5.3 ± 0.67	12.7 ± 0.5	8.8 ± 0.4	60.98 ± 1.39	3.58 ± 0.34	2.08 ± 0.34	55.62 ± 7.31
163800[v]	3.69 ± 0.82	2.38 ± 0.78	6.85 ± 0.3	5.16 ± 0.4	34.36 ± 2.16	2.31 ± 0.23	1.55 ± 0.24	38.5 ± 5.08
164794[v]	1.55 ± 0.40	1 ± 0.65	2.29 ± 0.54	1.83 ± 0.34	11.86 ± 2.47			
169454[v]	4.89 ± 0.85	2.99 ± 0.72	8.51 ± 0.54	6.47 ± 0.43	42.9 ± 2.79	2.76 ± 0.22	2.07 ± 0.31	48.74 ± 5.9
170740[v]	2.15 ± 0.43	1.73 ± 0.31	5.1 ± 0.29	2.84 ± 0.2	22.02 ± 0.57	1, 00 ± 0.23	0.76 ± 0.37	17.79 ± 6.76
172028[b]	5.05 ± 0.50	4.09 ± 0.35			47.83 ± 3.44	2.92 ± 0.16	1.79 ± 0.16	
210121[b]	4.45 ± 0.38	3.03 ± 0.23			26.65 ± 2.25	1.28 ± 0.06	1.23 ± 0.13	

We also present column densities of CH molecule obtained on the basis of BX (0,0) and (1,0) bands [10^{12} cm^{-2}]. We refer to the following data from the literature: a – Welty *et al.* (2020) , b – Bhatt and Cami (2015). Observational data from UVES are designed with *v*.

In Table 3 we present measured equivalent widths of OH band (centered near 3078 Å and 3082 Å) and CH B–X (0,0) and (1,0) bands (centered near 3886 Å and 3890 Å and near 3633 Å and 3636 Å, respectively). We also present calculated

column densities of CH on the basis of B–X (0,0) and (1,0) bands. In case of HD 147933, HD 172028, HD 210121 we used data on OH(A–X) and CH B–X (1,0) bands from the publication of Bhatt and Cami (2015) after precisely checking equivalent width ratio of lines based on oscillator strengths presented in Table 1.

Table 5 we presents calculated Pearson's correlation coefficients with errors used in data analysis performed in the case of each relation presented in Figs. 2–5. A standard error of the Pearson's correlation coefficient R (when $N_{\rm calc}$ of data points were used in data analysis) was estimated from the formula, $\sigma_R=(1-R^2)/\sqrt{N_{\rm calc}-1}$ (Fisher and Yates 1963). We also present critical values of the Pearson's correlation coefficient based on the Fisher and Yates (1963) statistical tables at the level of confidence 0.01 and result of the null hypothesis test $H_0 : \rho \geqslant 0$.

3. Results and Discussion

In Fig. 1 we present comparison of our measurements of OH features at 3078 Å and 3082 Å with those of Bhatt and Cami (2015). Generally results are consistent even though the features of interstellar OH are very weak in most cases.

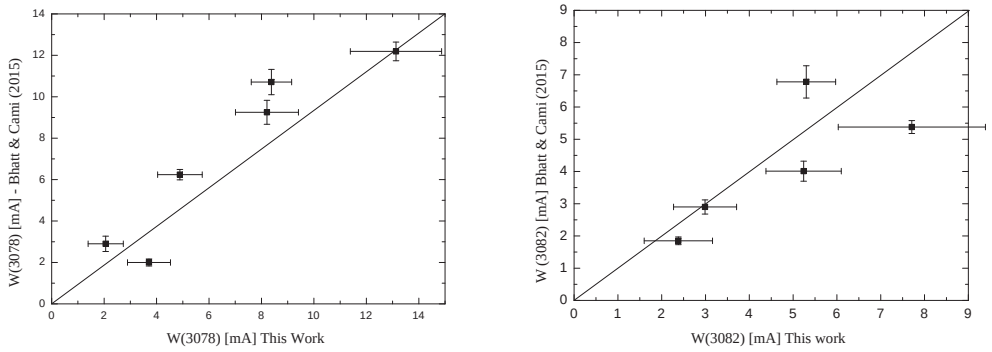

Fig. 1. Comparison of measurements of OH equivalent widths at 3078 Å and 3082 Å with those of Bhatt and Cami (2015).

Fig. 2 (left panel) shows the relation between equivalent widths of OH lines near 3078 Å and 3082 Å. The strength ratio, according to values of oscillator strengths published by Yousefi *et al.* (2018), *i.e.*, 0.001007 and 0.0006226, should be equal to 1.605. Fig. 2 demonstrates that the equivalent width ratio matches exactly that of the oscillator strengths with correlation coefficient equal to 0.98.

To obtain column densities we used the relation of Herbig (1968) which gives proper column densities when the observed lines are unsaturated:

$$N = 1.13 \times 10^{20} W_\lambda / (\lambda^2 f), \qquad (1)$$

where W_λ and λ are in Å and column density in cm^{-2}. To obtain column density we adopted f-values listed in Table 1.

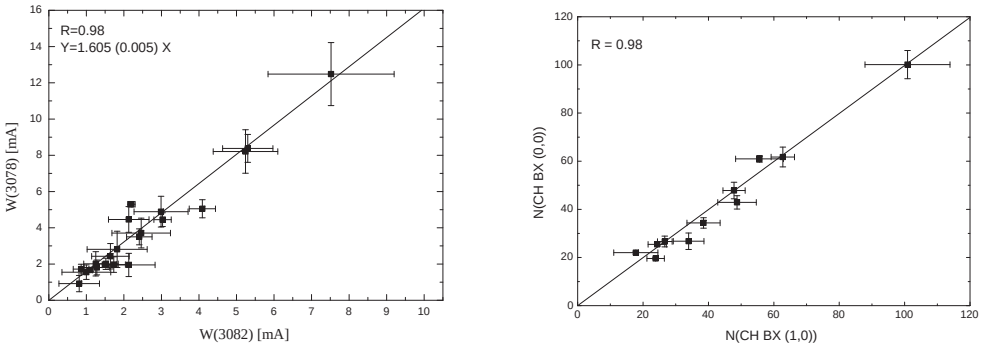

Fig. 2. *Left:* Correlation plot between equivalent widths of 3078 Å and 3082 Å lines of interstellar OH as measured in our spectra. This ratio, equal to 1.605 ± 0.005 matches the theoretical expectation based on recently published oscillator strengths.
Right: Correlation plot between column densities of CH molecule obtained on the basis of the BX (0,0) and BX (1,0) bands.

Column density of OH molecule was obtained as a sum of column densities from two transitions at 3078 Å and 3082 Å. To obtain column densities of CH we used unsaturated B–X (0,0) and B–X (1,0) features near 3886 Å and 3890 Å and near 3633 Å and 3636 Å, respectively. In Fig. 2 (right panel) we present correlation plot between column densities of CH molecule obtained on the basis of the B–X (0,0) and B–X (1,0) bands. Fig. 2 demonstrates that column densities obtained on the basis of the B–X (0,0) and B–X (1,0) bands exactly agree with correlation coefficient equal to 0.98.

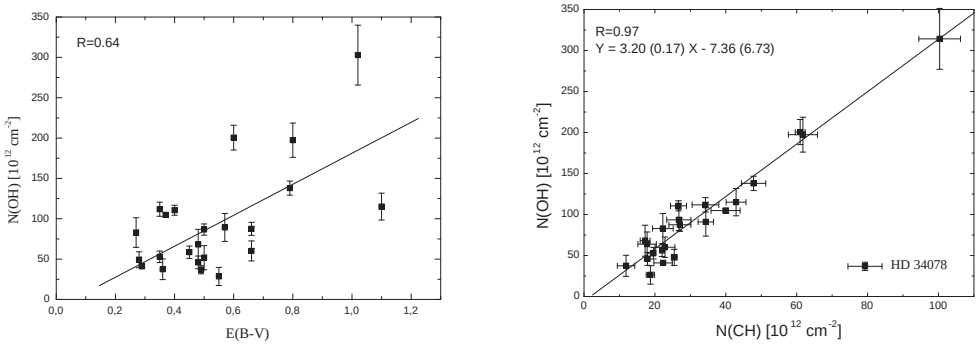

Fig. 3. *Left:* Relation between column densities of the OH molecule and interstellar reddening $E(B-V)$ with correlation coefficient equal to 0.64.
Right: Relation between column densities of the OH and CH molecules with correlation coefficient equal to 0.97 (HD 34078 was excluded).

In Fig. 3 (left panel) we present the relation between column densities of OH molecule and interstellar extinction $E(B-V)$. This relation, with correlation coefficient equal to 0.65, is rather good. This result, based on 24 objects, is consistent with that published previously by Weselak *et al.* (2009), *i.e.*, correlation coefficient equal to 0.68 based on 14 objects.

Fig. 3 (right panel) presents correlation between column densities of CH and OH radicals based on new oscillator strengths of OH A–X transitions at 3078 Å and 3082 Å. This relation (with one missing point excluded from correlation analysis, *i.e.*, HD 34078), based on 23 observations, is very good with correlation coefficient equal to 0.97. This relation suggests higher ratio of column densities of OH and CH, *i.e.*, 3.20 ± 0.17, as a result of new oscillator strengths of OH A–X transitions near 3078 Å and 3082 Å. Previously published value by Weselak *et al.* (2010b) was lower (*i.e.*, 2.52 ± 0.35). As a result of different oscillator strengths, column densities of OH molecule presented in Table 2 have higher values than published previously in the literature.

In Fig. 4 we present correlation plots between column density of the OH molecule and column densities of molecular and atomic hydrogen. The relation between abundances of OH and H_2 is much better than between OH and HI. This result, with correlation coefficient equal to 0.85, is based on 14 data-points. In Table 4 we present new column density ratios in the case of OH, CH and H_2 molecules with those published in the literature.

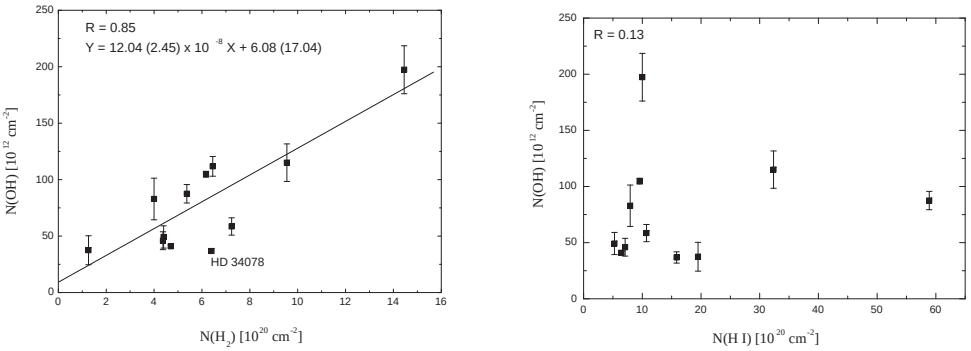

Fig. 4. Correlation patterns between column densities of OH molecule H_2 (*left*), HI (*right*). The best relation is that between column densities of OH and H_2 (correlation coefficient equal to 0.85).

Combining column densities of OH molecule from Roueff (1996) and Felenbok and Roueff (1996) with measurements of H_2 abundances from Savage *et al.* (1977), Rachford *et al.* (2002) and Joseph *et al.* (1986), Liszt and Lucas (2002) found abundance ratio of OH and H_2 molecules equal to $(1.0 \pm 0.2) \times 10^{-7}$ and OH and CH equal to 3.0 ± 0.9. Weselak *et al.* (2010b) found relation between abundances of OH and H_2 based on absorption–line observations toward five objects $(1.05 \pm 0.24) \times 10^{-7}$ and relation between abundances of OH and CH (2.52 ± 0.35) based on 16 objects. Relation between interstellar OH and H_2 molecules was also presented by Nguyen *et al.* (2018). For 16 molecular sightlines the abundance ratio of OH and H_2 was proven to be 1.0×10^{-7}. Result on the abundance ratio of OH and H_2 presented in this paper is close to that obtained by Rugel *et al.* (2018) (1.3×10^{-7}) on the basis of abundance estimation of H_2 from ^{13}CO(1–0) in the

T a b l e 4

Column density ratios of diatomic molecules presented in the literature compared with averaged values obtained in this work

Molecular column density ratio	Literature	This work
OH/CH	3.0 ± 0.9 [a]	3.20 ± 0.17
	2.52 ± 0.35 [b]	
OH/H_2	$(1.0 \pm 0.2) \times 10^{-7}$ [a]	$1.20 \pm 0.24 \times 10^{-7}$
	1.0×10^{-7} [c]	
	1.3×10^{-7} [d]	

a – Liszt and Lucas (2002), b – Weselak *et al.* (2010b), c – Nguyen *et al.* (2018), d – Rugel *et al.* (2018).

first Milky Way quadrant. The values presented in Table 4 prove that various methods toward targets inside and Galactic plane reproduce similar abundance ratios of interstellar molecules.

Finally, in Fig. 5 we present relation between equivalent widths of strong 5780 and 5797 DIBs and column densities of OH molecule. This relation was not presented previously. The better relation (with correlation coefficient equal to 0.52) is observed in the case of the 5797 DIB, which is also well correlated with column densities of CH (Friedman 2011, Weselak 2019). Thus, in comparison to wider 5780 the narrower 5797 DIB is better correlated with CH and OH. However, this result should be confirmed with additional observational material (based on Table 5 the relation between intensities of the 5797 DIB and column densities of OH molecule is statistically significant at the level of confidence higher than 0.02).

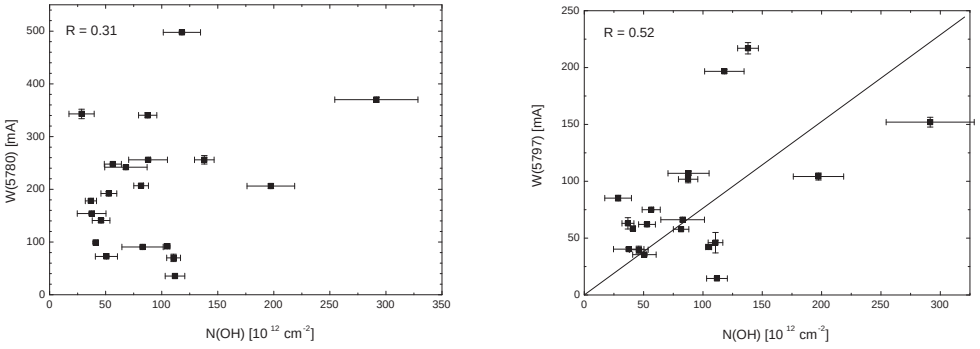

Fig. 5. Equivalent widths of the 5780 DIB (*left*) and 5797 DIB (*right*) correlated with column densities of OH. Better relation is seen in the case of the 5797 DIB (correlation coefficient equal to 0.52).

T a b l e 5

Pearson's correlation analysis

Relation	R	σ_R	$N_{\rm calc}$	ρ	Result
W(3078) *vs.* W(3082)	0.98	0.08	23	0.51	+
N(CH BX 00) *vs.* N(CH BX 10)	0.98	0.01	11	0.68	+
N(OH) *vs.* $E(B-V)$	0.64	0.12	24	0.50	+
N(OH) *vs.* N(CH)	0.97	0.01	23	0.51	+
N(OH) *vs.* N(H_2)	0.85	0.08	14	0.62	+
N(OH) *vs.* N(HI)	0.13	0.26	15	0.61	–
W(5780) *vs.* N(OH)	0.31	0.21	20	0.54	–
W(5797) *vs.* N(OH)	0.52	0.17	19	0.55	–

R – Pearson's correlation coefficient, σ_R – its error, $N_{\rm calc}$ – number of stars, ρ – critical value of the correlation coeficient, Result – significance the correlation

4. Conclusions

The above considerations allow us to infer the following conclusions:

1. The column density of OH is well correlated with interstellar reddening $E(B-V)$.

2. The column density of OH is very well correlated with interstellar CH. This result is based on more numerous sample of objects and new values of oscillator strengths of OH A–X transitions at 3078 Å and 3082 Å.

3. The column density of OH is very well correlated with interstellar H_2. This result is based on more numerous sample of objects and new values of oscillator strengths of OH A–X transitions.

4. The narrower 5797 DIB is better correlated with OH molecule than the 5780 DIB. This relation is statistically significant at the level of confidence greater than 0.02.

It is difficult to answer the question whether narrow DIBs as 5797 are rather connected to the chemistry of oxygen-bearing molecules or carbon-rich network. More numerous sample of objects in case of OH molecule is required to perform further analysis and answer this question.

Acknowledgements. The author is grateful to the anonymous referee for valuable suggestions that allowed him to improve the final version of the manuscript.

REFERENCES

Bagnulo, S., Jehin, E., Ledoux, C., *et al.* 2003, *The Messenger*, **114**, 10.
Benz, A.O., Bruderer, S., van Dishoeck, E.F., *et al.* 2010, *A&A*, **521**, L35.
Bhatt, N.H., and Cami, J. 2015, *ApJS*, **216**, 22.
Blake, G.A., Keene, J., and Philips, T.G. 1985, *ApJ*, **295**, 501.
Boissé, P., Le Petit, F., Rollinde, E., *et al.* 2005, *A&A*, **429**, 509.
Chaffee, F.H., Jr., and Lutz, B. 1977, *ApJ*, **213**, 394.
Cox, N.L.J., Cami, J., Farhang, A. *et al.* 2017, *A&A*, **606**, 76.
Crutcher, R.M., and Watson, W.D. 1976, *ApJ*, **209**, 778.
De Luca, M., Gupta, H., Neufeld, D., *et al.* 2012, *ApJ*, **751**, L37.
Diplas, A., and Savage, B.D. 1994, *ApJS*, **93**, 211.
Douglas, A.E., and Herzberg 1941, *ApJ*, **94**, 381.
Fan, H., Welty, D.E., York, D.G., *et al.* 2017, *ApJ*, **850**, 194.
Federman, S.R. 1982, *ApJ*, **257**, 125.
Felenbok, P., and Roueff, E. 1996, *ApJ*, **465**, L57.
Fisher, R.A., and Yates, F. 1963, in: "Statistical Tables for Biological, Agricultural, and Medical Research".
Fitzpatrick, E.L., and Massa, D. 1990, *ApJS*, **72**, 163.
Friedman, S.D., York, D.G., McCall, B.J., *et al.* 2011, *ApJ*, **727**, 33.
Galazutdinov, G.A. 1992, *Prep. Spets. Astrof. Obs.*, 92.
Gerin, M., Neufeld, D.A., and Goicoechea, J.R. 2016, *Ann. Rev. Astron. Astrophys.*, **54**, 181.
Gredel, R., van Dishoeck, E.F., and Black, J.H. 1993, *A&A*, **269**, 477.
Heger, M.L. 1922, *Lick Obs. Bull.*, **10**, 146.
Herbig, G.H. 1968, *Zeitschrift für Astrophysik*, **68**, 243.
Hobbs, L.M., York, D.G., Thorburn, J.A., *et al.* 2009, *ApJ*, **705**, 32.
Joseph, C.L., Snow, T.P. Jr., Seab, C.G., and Crutcher, R.M. 1986, *ApJ*, **309**, 771.
Lien, D.J. 1984, *ApJ*, **284**, 578.
Liszt, H., and Lucas, R. 2002, *A&A*, **391**, 693.
Mattila, K. 1986, *A&A*, **160**, 157.
McKellar, A. 1940a, *PASP*, **52**, 187.
McKellar, A. 1940b, *PASP*, **52**, 312.
Meyer, D.M., and Roth, K.C. 1991, *ApJ*, **376**, L49.
Neufeld, D.A., Zmuidzinas, J., Schilke, P., *et al.* 1997, *ApJ*, **488**, L141.
Neufeld, D.A., Roueff, E., Snell, R.L., *et al.* 2012, *ApJ*, **748**, 37.
Nguyen, H., Dawson, J.R., Miville-Deschenes, M.A., *et al.* 2018, *ApJ*, **862**, 49.
Pan, K., Federman, S.R., Cunha, K., Smith, V.V., and Welty, D.E. 2004, *ApJS*, **151**, 313.
Rachford, B.L., Snow, T.P. Tumlinson, J., *et al.* 2001, *ApJ*, **555**, 839.
Rachford B.L., Snow, T.P., Tumlinson, J., *et al.* 2002, *ApJ*, **577**, 221.
Rachford B.L., Snow, T.P., Destree, J.D.*et al.* 2009, *ApJS*, **180**, 125.
Roueff, E. 1996, *MNRAS*, **279**, L37.
Rugel, M.R., Beuther, H., Bihr, S., *et al.* 2018, *A&A*, **618**, 159.
Savage, B.D., Bohlin, R.C., Drake, J.F., and Budich, W. 1977, *ApJ*, **216**, 291.
Schilke, P., Benford, D.J., Hunter, T., Lis, D.C., and Phillips, T.G. 2001, *ApJS*, **132**, 281.
Schilke, P., Neufeld, D.A., Muller, H.S.P., *et al.* 2014, *A&A*, **566**, A29.
Sheffer, Y., Rogers, M., Federman, S.R., *et al.* 2007, *ApJ*, **667**, 1002.
Sheffer, Y., Rogers, M., Federman, S.R., *et al.* 2008, *ApJ*, **687**, 1075.
Snow, T.P. 1996, *ApJ*, **465**, 245.
Snow, T.P., Ross, T.L., Destree, J.D., *et al.* 2008, *ApJ*, **688**, 1124.
Swings, P., and Rosenfeld, L. 1937, *ApJ*, **86**, 483.
Weinreb, S., Barrett, A.H., Meeks, M.L., and Henry, J.C. 1963, *Nature*, **200**, 829.
Welty, D.E., Sonnentrucker, P., Snow, T.P., and York, D.G. 2020, *ApJ*, **897**, 36.

Weselak, T., Galazutdinov, G.A., Musaev, F.A., and Krełowski, J. 2008, *A&A*, **484**, 381.
Weselak, T., Galazutdinov, G.A., Beletsky, Y., and Krełowski, J. 2009, *A&A*, **499**, 783.
Weselak, T., Galazutdinov, G.A., Han, I., and Krełowski, J. 2010a, *MNRAS*, **401**, 1308.
Weselak, T., Galazutdinov, G.A., Beletsky, Y., and Krełowski, J. 2010b, *MNRAS*, **402**, 1991.
Weselak, T., Galazutdinov, G.A., Beletsky, Y., and Krełowski, J. 2011, *Astron. Nachr.*, **332**, 167.
Weselak, T., Galazutdinov, G.A., Gnaciński, P., and Krełowski, J. 2014, *Acta Astron.*, **64**, 277.
Weselak, T. 2019, *A&A*, **625**, 55.
Weselak, T. 2020, *Acta Astron.*, **70**, 301.
Wyrowski, F., Menten, K.M., Gunsten, R., *et al.* 2010, *A&A*, **518**, A26.
Yousefi, M., Bernath, P., Hodges, J., *et al.* 2018, *Journal of Quantitative Spectroscopy and Radiative Transfer*, **217**, 416.